

Luminescence Properties of $\text{CaAl}_2\text{O}_4:\text{Eu}^{3+}$, Gd^{3+} Phosphors Synthesized by Combustion Synthesis Method

N. VERMA^{a,*}, K.C. SINGH^a, B. MARÍ^b, M. MOLLAR^b, J. JINDAL^a

^aDepartment of Chemistry, Maharshi Dayanand University, Rohtak 124001, Haryana, India

^bInstitut de Disseny per la Fabricació Automatitzada, Departament de Física Aplicada, Universitat Politècnica de València, Camí de Vera s/n, 46022 València, Spain

(Received August 22, 2016; in final form October 9, 2017)

$\text{CaAl}_2\text{O}_4:\text{Eu}^{3+}$ (1 mol.%) co-doped with varying concentration of Gd^{3+} (1, 2, 5, and 10 mol.%) were prepared by combustion synthesis method at 600 °C and further annealed at 1000 °C. All the compositions were investigated for their structural and photoluminescence properties. It was observed that both states of europium i.e. Eu^{3+} and Eu^{2+} were present and ratio of these states changes on heating at 1000 °C. The materials synthesized at 600 °C showed high intense peak around 440 nm due to presence of Eu^{2+} and less intense peaks in the red region which were due to presence of Eu^{3+} . On annealing the compounds at 1000 °C, intensity of peak around 440 nm decreases and intensity of peaks in the red region increases significantly. The ${}^5D_0 \rightarrow {}^7F_3$ transition due to Eu^{3+} at 657 nm appears as the highest intensity peak. All co-doped samples annealed at 1000 °C showed the higher intensity than the mono doped sample which is due to energy transfer from the Gd^{3+} to Eu^{3+} . The second rare-earth ion (Gd^{3+}) acts as sensitizer and enhances the photoluminescence intensity. The X-ray diffraction spectra reveal the monoclinic phase of CaAl_2O_4 in all the samples which showed that Eu^{3+} and Gd^{3+} do not change the crystalline structure of calcium aluminate.

DOI: [10.12693/APhysPolA.132.1261](https://doi.org/10.12693/APhysPolA.132.1261)

PACS/topics: phosphors, luminescence, combustion method, calcium aluminate

1. Introduction

The synthesis of inorganic luminescent materials is an area of great interest [1–7]. This area have attracted much attention due to the unique properties of luminescent materials particularly applied in light emitting devices like color displays, plasma display panels, fluorescent lamps, fiber amplifiers etc. [8–11]. Inorganic luminescent materials are also widely used for solar cells for enhancing sunlight harvesting to increase the efficiency of solar cells [12–14]. These luminescent materials are synthesized by doping of rare earth (RE) ions into host lattices. Among luminescent materials, alkaline earth aluminates MAl_2O_4 (where M = Ca, Sr, Ba) doped with various kinds of RE ions or other metal ions (M^+ or M^{2+} or M^{3+}) show strong luminescence properties in the visible region. Aluminate-based phosphors have good thermal and chemical stability [15]. The other benefit of using alkaline earth aluminates as the host lattice specially CaAl_2O_4 , is its long persistence, which is highly applicable in optical devices like luminous paints on highways on airports and buildings [16, 17].

The phosphors with a long after glow have important application in the display devices. The long persistent glow can be improved by co-doping of certain rare-earth ions like Gd^{3+} , Nd^{3+} etc. The $\text{CaAl}_2\text{O}_4:\text{Eu}^{2+}$, Gd^{3+} phosphor is one kind of the long after glow phosphors.

In these phosphors, Eu^{2+} ions play the role of activators, whereas Gd^{3+} ions generated hole traps that resulted in the long persistent phosphorescence and also act as a sensitizer in the phosphor [18, 19]. The concentration of Gd^{3+} ion as co-dopant has strong influence on the luminescence time and luminescence intensity of phosphor. $\text{CaAl}_2\text{O}_4:\text{Eu}^{2+}$ co doped with Nd^{3+} has been reported with very high after glow as compare to mono doped $\text{CaAl}_2\text{O}_4:\text{Eu}^{2+}$ [20]. The lifetime of luminescence of co-doped materials increases as compared to singly doped materials. CaAl_2O_4 doped with Eu^{2+} prepared by combustion synthesis method was reported [21] showing good luminescent properties in blue-green region. The $\text{SrAl}_2\text{O}_4:\text{Eu}^{2+}$ co-doped with Dy^{3+} and Yb^{3+} shows that there is an increase of photoluminescence intensity with increase in Yb^{3+} concentration [22]. Similarity among ionic radii of Ca^{2+} (1.26 Å), Eu^{3+} (1.206 Å) and Eu^{2+} (1.16 Å) make the CaAl_2O_4 a promising host lattice for Eu^{3+} or Eu^{2+} ion [21, 23]. Europium can be incorporated into CaAl_2O_4 lattice in Eu^{3+} or Eu^{2+} or both valence states together [24]. There are various methods to prepare these rare earth doped compounds like solid state reaction, combustion reaction, hydrothermal method, precipitation method, micro emulsion method, microwave method, sol gel synthesis method [25–31].

In this paper, we report our investigations on photoluminescence properties of nanocrystalline $\text{CaAl}_2\text{O}_4:\text{Eu}^{3+}:\text{Gd}^{3+}$ materials synthesized by combustion method. This method provides an interesting alternative over other elaborated techniques because it offers several attractive advantages such as: simplicity of experimental setup; surprisingly short time between the

*corresponding author; e-mail: vermanaveen17@gmail.com

preparation of reactants and the availability of the final product. The obtained materials are crystalline and may be applied in the field of photovoltaic as a down shifting material and in the fabrication of light emitting devices.

In this study, we observed the effect of Gd^{3+} co-doping on structural and luminescence properties of $CaAl_2O_4:Eu^{3+}$ (1 mol.%) compound. The effect of annealing is also studied on the existence of prominent valence state of europium (Eu^{2+}/Eu^{3+}) in $CaAl_2O_4:Eu$. Powder X-ray diffraction is used for phase and crystalline structure determination. Photoluminescence characteristics were studied by excitation of powder material by 325 nm laser radiation.

2. Experimental

The combustion synthesis method was used to prepare $CaAl_2O_4:Eu^{3+}, Gd^{3+}$ with varying concentration of Gd^{3+} (1, 2, 5, and 10 mol.%). The Eu^{3+} concentration were kept fixed at 1 mol.% for all compositions. High-purity $[Ca(NO_3)_2]$, $[Al(NO_3)_3]$, $[Eu(NO_3)_3]$, $[Gd(NO_3)_3]$ and urea from Sigma Aldrich were used as starting material. Materials in their stoichiometric ratio for the formation of $CaAl_2O_4:Eu^{3+}:Gd^{3+}$ complexes were taken and mixed with a calculated amount of urea and a paste material was prepared by adding few drops of deionized water. The amount of urea was calculated using total oxidizing and reducing valencies [32]. The paste of mixture was transferred to preheated furnace at 600 °C. At high temperature material undergoes rapid dehydration, combustion and a voluminous solid is formed with the generation of combustible gases. The solid obtained is further annealed at 1000 °C for 3 h to increase the crystalline character.

The structural characterization was performed by high resolution X-ray diffraction (XRD) using Rigaku Ultima IV diffractometer in the $\theta-2\theta$ configuration with $Cu K_\alpha$ radiation (1.54184 Å). The morphology of the crystals was studied by scanning electron microscope (SEM) using JEOL JSM6300 model operating at 10 kV. Photoluminescence (PL) experiments were performed in backscattering geometry using a He–Cd laser (325 nm) with an optical power of 30 mW for excitation. The emitted light was analyzed by HR-4000 Ocean Optics USB spectrometer optimized for the UV–vis range. For photoluminescence measurements, 0.05 g powder samples were pressed into pellets (10 mm diameter and 1 mm thickness) and then exposed to a 325 nm He–Cd laser. All measurements were carried out at room temperature.

3. Results and discussion

3.1. XRD analysis

Figure 1a and b represents the XRD pattern of the $CaAl_2O_4:Eu(1\text{ mol.}\%):Gd^{3+}$ (1, 2, 5, 10 mol.%) as prepared at 600 °C and annealed at 1000 °C, respectively. From XRD patterns of $CaAl_2O_4:Eu(1\text{ mol.}\%):Gd^{3+}$ (1, 2, 5, 10 mol.%) powder materials it was observed that all

the samples show good crystalline behavior with monoclinic $CaAl_2O_4$ as the main phase and the same structure is retained after doping of Eu^{3+} (1 mol.%) and Gd^{3+} (1, 2, 5, and 10 mol.%) which showed that the introduction of RE ions did not alter the crystal structure of host lattice. All the peaks were identified and well matched with $CaAl_2O_4$ [JCPDS No 001-0888]. The peaks corresponding to Gd_2O_3 were found due to formation of separate phase and that appears with Gd^{3+} concentration higher than 2 mol.%. The peaks correspond to Gd_2O_3 arise at 2θ 29.11° and 51.88° [JCPDS card no. 024-0430] while peaks for Al_2O_3 were detected (Fig. 1) at 2θ 36.81° and 59.38° [JCPDS 023-1009]. The peak due to $CaAl_2O_4$ at 37.30° merged with Al_2O_3 peak at 36.81°. The Eu^{3+} (1.20 Å), Eu^{2+} (1.20 Å), Gd^{3+} (0.93 Å) all occupies Ca^{2+} (1.26 Å) sites due to almost similar radii [33]. The crystallite size was calculated by the Debye–Scherrer relation using Gaussian fitting for the most intense peak (220) at 30.18° in the XRD pattern. The crystallite size for all samples was found in the 40–45 nm range. Co-doping of Gd^{3+} ion and annealing did not show any significant effect on crystallite size.

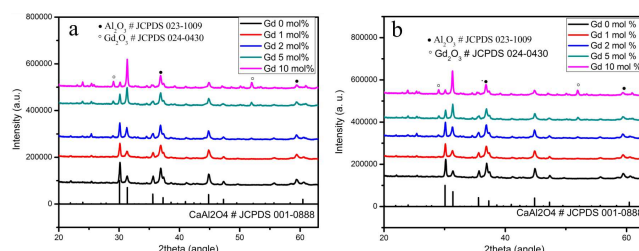


Fig. 1. XRD pattern for $CaAl_2O_4:Eu^{3+}, Gd^{3+}$ (1, 2, 5 and 10 mol.%) as prepared at 600 °C (a) and annealed at 1000 °C.

3.2. SEM analysis

SEM images of $CaAl_2O_4:Eu^{3+}:Gd^{3+}$ samples are shown in Fig. 2. The images show particle clusters and flaky aggregates. SEM images clearly indicate the presence of grains with non uniform shape and sizes. This might be due to unequal distribution of temperature and mass flow in the combustion flame. This observed morphology is consistent with combustion derived products compounds [15]. The flakes also have porosity with different dimensions. Several pores are observed in SEM image which are formed by the escaping gases during the combustion reaction. Also, several small particles can be seen within grains.

3.3. Photoluminescence properties of $CaAl_2O_4:Eu^{3+}:Gd^{3+}$

The photoluminescence spectra of $CaAl_2O_4:Eu^{3+}:Gd^{3+}$ (1, 2 and 5 mol.%) as prepared materials at 600 °C and samples annealed at 1000 °C are shown in Fig. 3a and b, respectively. PL emission spectra of all prepared compounds showed the presence of both valence

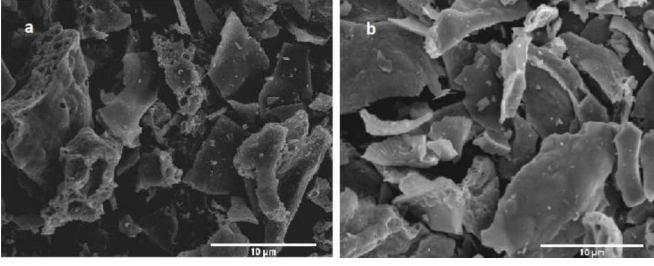


Fig. 2. SEM micrographs for $\text{CaAl}_2\text{O}_4:\text{Eu}^{3+}$, Gd^{3+} : 1 mol.% (a) and 5 mol.% (b).

states of europium ($\text{Eu}^{2+}/\text{Eu}^{3+}$). It has been observed that in some special type of lattices where the reduction of $\text{Eu}^{3+} \rightarrow \text{Eu}^{2+}$ could occur when the compounds were prepared in air. Some of the reported lattices for this type of reduction are SrB_4O_7 [33], $\text{Sr}_4\text{Al}_{14}\text{O}_{25}$ lattice [34], $\text{BaB}_8\text{O}_{13}$ [35], $\text{Ba}_3(\text{PO}_4)_2$ [36]. We observed this $\text{Eu}^{3+} \rightarrow \text{Eu}^{2+}$ reduction in the $\text{CaAl}_2\text{O}_4:\text{Eu}^{3+}:\text{Gd}^{3+}$ compounds which may be due to charge compensation [37]. When trivalent Eu^{3+} was doped into CaAl_2O_4 , they would replace the Ca^{2+} ions of CaAl_2O_4 . For keeping the charge balance three Ca^{2+} should be replaced by two Eu^{3+} . Hence one vacancy defect is created with two negative charge, and two positive defects (Eu_{Ca}) were created due to replacement of Eu^{3+} in lattice of CaAl_2O_4 . The vacancy defect may act as donor and Eu_{Ca} defect act as acceptor. Consequently, by thermal stimulation the electron is transferred from the vacancy defect to Eu_{Ca} sites and there is the reduction of Eu^{3+} to Eu^{2+} . The more electrons released by negative defects were created, the more Eu^{3+} ions would be reduced to Eu^{2+} .

Figure 3a shows the photoluminescence spectrum of $\text{CaAl}_2\text{O}_4:\text{Eu}^{3+}$ (1 mol.%): Gd^{3+} (1–10 mol.%) phosphors prepared at 600°C by combustion synthesis method. The photoluminescence curves showed the presence of both Eu^{2+} and Eu^{3+} valence state of europium. The curves show a broad emission peak in the blue-green region at 441.5 nm due to Eu^{2+} and other peaks at 576 (${}^5D_0 \rightarrow {}^7F_0$), 587 (${}^5D_0 \rightarrow {}^7F_1$), 614 (${}^5D_0 \rightarrow {}^7F_2$), 657 (${}^5D_0 \rightarrow {}^7F_3$), 681, 703 (${}^5D_0 \rightarrow {}^7F_4$) nm due to Eu^{3+} ion in the crystal lattice of CaAl_2O_4 . This emission at 441.5 nm in the blue-green region arises due to a typical $4f^65d^1$ to $4f^7$ transition of Eu^{2+} ion. The emission intensity of this peak decreases with increase in Gd^{3+} concentration and almost diminishes when concentration of Gd^{3+} was 10 mol.%. This decrease in intensity is compensated by increase in intensity of peaks near 657 nm due to the presence of Eu^{3+} (Fig. 3a) when the concentration of Gd^{3+} increases from 0 to 2 mol.%, the peak intensity due to Eu^{2+} at 441.5 nm decreases, and that decrease in intensity is compensated by the increase in intensities of peaks due to Eu^{3+} . On further increase of the concentration of Gd^{3+} due to concentration quenching there is a decrease in intensity of both the peaks. The increase in intensity of photoluminescence at 657 nm and decrease

in intensity of peak situated at 441.5 nm showed that the Gd^{3+} introduction increases the overall red emission of the phosphor and decreases the blue green emission [38] which showed that Gd^{3+} act as emission wavelength tunable agent for the phosphor material. This increase in brightness indicates that the energy absorbed by Gd^{3+} ions can be transferred efficiently to Eu^{3+} due to some energy matching so Gd^{3+} perform the function of sensitizer as explained above. This type of energy transfer between Gd^{3+} and Eu^{3+} was also reported earlier [39]. This shows the energy transfer through cross-relaxation from Gd^{3+} to Eu^{3+} .

The reported work [38] also observed two peaks due to Gd^{3+} at 273 and 311 nm, which were attributed to the ${}^8S_{7/2} \rightarrow {}^6I_J$ and ${}^8S_{7/2} \rightarrow {}^6P_J$ transitions, respectively. These types of emission peaks corresponding to Gd^{3+} are also observed in earlier reported articles [40]. This energy can be transferred to Eu^{3+} in the sample and consequently increase the photoluminescence intensity. The maximum intensity was observed for $\text{CaAl}_2\text{O}_4:\text{Eu}^{3+}$ (1 mol.%) Gd^{3+} (1 mol.%) compound (Fig. 3b) which was threefold as that of non co-doped $\text{CaAl}_2\text{O}_4:\text{Eu}^{3+}$ (1 mol.%) compound. All compounds with co-doping of Gd^{3+} have higher intensity than non co-doped $\text{CaAl}_2\text{O}_4:\text{Eu}^{3+}$ (1 mol.%) compound.

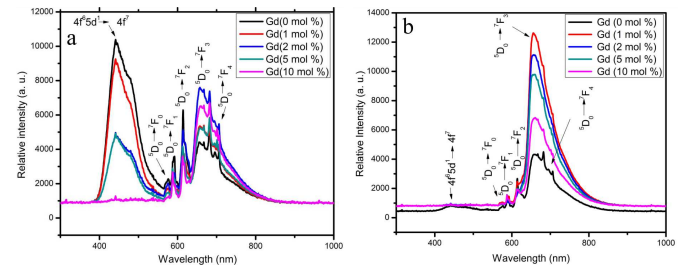


Fig. 3. PL emission spectra for $\text{CaAl}_2\text{O}_4:\text{Eu}^{3+}, \text{Gd}^{3+}$ (1, 2, 5 and 10 mol.%) as prepared at 600°C ($\lambda_{\text{exc}} = 325$ nm) (a) and annealed at 1000°C ($\lambda_{\text{exc}} = 325$ nm) (b).

4. Conclusion

$\text{CaAl}_2\text{O}_4:\text{Eu}^{3+}$ compounds co-doped with varying concentration Gd^{3+} were synthesized by combustion synthesis method. The X-ray diffraction study shows the retaining of monoclinic phase of CaAl_2O_4 on doping of Eu^{3+} and co-doping of Gd^{3+} which showed that the crystal structure remains unaffected by introduction of RE ions. With the change in concentration of co-dopant (Gd^{3+}) the ratio of peaks intensities due to Eu^{2+} and Eu^{3+} changes. Thus changing concentration of co-dopant is expected to provide a means to tune the emission spectrum of RE doped aluminates. As prepared material showed most intense peak around 440 nm due to Eu^{2+} which on annealing at 1000°C diminished due to oxidation of Eu^{2+} to Eu^{3+} . In the annealed compounds, highest intense peak is due to the ${}^5D_0 \rightarrow {}^7F_3$ transition in the red

region at 657 nm due to Eu^{3+} . It was found that due to sensitizing effect of Gd^{3+} co-doped materials showed higher PL intensity as compared to CaAl_2O_4 mono doped with Eu ion.

Acknowledgments

This work was supported by the Generalitat Valenciana through grant PROMETEUS 2009/2013 and the European Commission through Nano CIS project (FP7-PEOPLE-2010-IRSES ref. 269279).

References

- [1] L. Gan, Z.Y. Mao, F.F. Xu, Y.C. Zhu, X.J. Liu, *Ceram. Int.* **40**, 5067 (2014).
- [2] J.T. Ingle, R.P. Sonekar, S.K. Omanwar, Y. Wang, L. Zhao, *J. Alloys Comp.* **608**, 235 (2014).
- [3] O. Annalakshmi, M.T. Jose, B. Venkatraman, G. Amarendra, *Mater. Res. Bull.* **50**, 494 (2014).
- [4] Y. Kaur, V. Parganiha, D. Dubey, D. Singh, *Superlatt. Microstruct.* **73**, 38 (2014).
- [5] E. Shafia, M. Bodaghi, S. Esposito, A. Aghaei, *Ceram. Int.* **40**, 4697 (2014).
- [6] B. Marí, K.C. Singh, M. Sahal, S.P. Khatkar, V.B. Taxak, M. Kumar, *J. Lumin.* **131**, 587 (2011).
- [7] B. Marí, K.C. Singh, M. Sahal, S.P. Khatkar, V.B. Taxak, M. Kumar, *J. Lumin.* **130**, 2128 (2010).
- [8] P. Thiyagarajan, M. Kottaisamy, K. Sethupathi, M.S.R. Rao, *Displays* **30**, 202 (2009).
- [9] J.T. Ingle, R.P. Sonekar, S.K. Omanwar, Y. Wang, L. Zhao, *Opt. Mater.* **36**, 1299 (2014).
- [10] D.S. Zang, J.H. Song, D.H. Park, Y.C. Kim, D.H. Yoon, *J. Lumin.* **129**, 1088 (2009).
- [11] A.A. Reddy, S.S. Babu, G.V. Prakash, *Opt. Commun.* **285**, 5364 (2012).
- [12] H. Yoshida, N. Sato, *J. Phys. Chem. C* **116**, 10333 (2012).
- [13] H. Lian, Z. Hou, M. Shang, D. Geng, Y. Zhang, J. Lin, *Energy* **57**, 270 (2013).
- [14] U. Rambabu, S.D. Han, *Ceram. Int.* **39**, 1603 (2013).
- [15] T. Aitasalo, J. Holsa, H. Jungner, M. Lastusaari, J. Niittykoski, *J. Phys. Chem. B* **110**, 4589 (2006).
- [16] K. Van den Eeckhout, P.F. Smet, D. Poelman, *Materials* **3**, 2536 (2010).
- [17] T. Aitasalo, J. Holsa, H. Jungner, M. Lastusaari, J. Niittykoski, *J. Alloys Comp.* **341**, 76 (2002).
- [18] P. Docampo, T. Bein, *Acc. Chem. Res.* **49**, 339 (2016).
- [19] H. Ryu, K.S. Bartwal, *J. Phys. D Appl. Phys.* **41**, 235404 (2008).
- [20] Phosphorescent Phosphor US patent 5424006. 1995.
- [21] R.H. Krishna, B.M. Nagabhushana, H. Nagabhushana, R.P.S. Chakradhar, N.S. Murthy, R. Sivaramakrishna, C. Shivakumara, J.L. Rao, T. Thomas, *J. Alloys Comp.* **589**, 596 (2014).
- [22] R. Chen, Y. Wang, Y. Hu, Z. Hu, C. Liu, *J. Lumin.* **128**, 1180 (2008).
- [23] V. Singh, J.J. Zhu, M.K. Bhide, V. Natarajan, *Opt. Mater.* **30**, 446 (2007).
- [24] S. Janakova, L. Salavcova, G. Renaudin, Y. Filinchuk, D. Boyer, P. Boutinaud, *J. Phys. Chem. Solids* **68**, 1147 (2007).
- [25] Y. Wu, Z. Sun, K. Ruan, Y. Xu, H. Zhang, *J. Lumin.* **155**, 269 (2014).
- [26] B. Marí, K.C. Singh, P.C. Coca, I. Singh, D. Singh, S. Chand, *Displays* **34**, 346 (2013).
- [27] B. Marí, K.C. Singh, M. Moya, I. Singh, H. Om, S. Chand, *Opt. Mater.* **34**, 1267 (2012).
- [28] X.F. Wang, G.H. Peng, N. Li, Z.H. Liang, X. Wang, J.L. Wu, *J. Alloys Comp.* **599**, 102 (2014).
- [29] X. Ju, X. Li, W. Li, W. Yang, C. Tao, *Mater. Lett.* **65**, 2642 (2011).
- [30] Y. Sun, G. Qiu, X. Li, S. Zhang, C. Yan, X. Zhang, *Rare Metals* **25**, 615 (2006).
- [31] A. Birkel, N.A. DeCino, N.C. George, K.A. Hazelton, B.C. Hong, R. Seshadri, *Solid State Sci.* **19**, 51 (2013).
- [32] S. Ekambaram, K.C. Patil, *J. Alloys Comp.* **248**, 7 (1997).
- [33] Z. Pei, Q. Su, J. Zhang, *J. Alloys Comp.* **198**, 51 (1993).
- [34] M. Peng, Z. Pei, G. Hong, Q. Su, *Chem. Phys. Lett.* **371**, 1 (2003).
- [35] L.H. Bin, H.T. Dou, W.S. Bin, Z.Q. Hua, P.Z. Wu, S. Qiang, *Chin. J. Chem.* **18**, 294 (2000).
- [36] I. Tale, P. Kulis, V. Kronghauz, *J. Lumin.* **20**, 343 (1979).
- [37] K.B. Kim, K.W. Koo, T.Y. Cho, H.G. Chun, *Mater. Chem. Phys.* **80**, 682 (2003).
- [38] US Patent 6827877 B2.
- [39] J. Zhong, H. Liang, Q. Sou, J. Zhou, Y. Huang, Z. Gao, Y. Tao, J. Wang, *Appl. Phys. B* **98**, 149 (2010).
- [40] V. Singh, G. Sivaramaiah, J.L. Rao, S.H. Kim, *J. Lumin.* **143**, 162 (2013).